

Robust Nuclear Observables and Constraints on Random Interactions

Dimitri Kusnezov^a, N.V. Zamfir^{b,c,d} and R.F. Casten^b

^a*Center for Theoretical Physics, Sloane Physics Lab, Yale University, New Haven, CT 06520-8120*

^b*Wright Nuclear Structure Laboratory, Yale University, New Haven, CT 06520-8120*

^c*Clark University, Worcester, Massachusetts 01610*

^d*National Institute for Physics and Nuclear Engineering, Bucharest-Magurele, Romania*
(November 9, 2018)

The predictions of the IBM two-body random ensemble are compared to empirical results on nuclei from $Z=8$ to 100. Heretofore unrecognized but robust empirical trends are identified and related both to the distribution of valence nucleon numbers and to the need for and applicability of specific, non-random interactions. Applications to expected trends in exotic nuclei are discussed.

Recently there has been renewed interest in the spectroscopic properties of Hamiltonians with random interactions [1–7]. Scrutiny has focused on nuclear systems but applications exist in other many body quantal systems such as quantum dots or metallic clusters. In the nuclear case, analyses have been carried out in the frameworks of the Shell Model [1–3,5] and the Interacting Boson Model (IBM) [4–6].

These studies are extremely important because they explore the origins of fundamental features of nuclear structure. The upshot of these studies has been surprising recognition that some of the most hallowed aspects of structure, such as 0^+ ground states for even-even nuclei, and even vibrational spectra, arise with randomly distributed interactions.

It is the purpose of this Letter to confront calculations with random and non-random interactions with robust experimental results to study which pervasive features of nuclei arise from the basis space and the generic type of interaction (e.g., 2-body) and which depend on the details of the interaction. We will use the insights developed in this analysis to better understand structural evolution and its relation to shell structure, and to project the behavior of exotic nuclei.

First, it is useful to succinctly summarize existing studies. In Shell model [1–3] and IBM [4–6] approaches for many-body systems, the majority (typically $\sim 70\%$) of calculated ground states have $J^\pi = 0^+$ even though 0^+ states comprise a much smaller fraction of the basis space than other angular momenta. While it might be suspected that such a "pairing" property could emerge as a consequence of time reversal invariance, it has been shown [2] that this is not the case. Comparison of ground state wave functions in nuclei differing by two nucleons shows [3] further evidence for a pairing relationship, reflecting the generalized seniority scheme [8]. The analysis also extends to excited states. In the Shell Model, modest probabilities were found [1] for vibration-like spectra, defined by energy level ratios $R_{4/2} \equiv E(4_1^+)/E(2_1^+)$ near 2.0. However it was not possible to produce significant numbers of spectra with rotational character, $R_{4/2} \sim 10/3$.

In the IBM analyses [4–6] a similar preponderance of 0^+ ground states was found. Here,

however, in contrast to the Shell Model, the interactions in an s-d boson space lead rapidly, with increasing boson number N_B , to large probabilities for both vibrational [$R_{4/2} \sim 2.0$] and rotational [$R_{4/2} \sim 3.33$] spectra. Indeed, the IBM treatments produced no concentrations of $R_{4/2}$ values near *any other* values, as noted in Refs. [4–6]. These results are reminiscent of empirical correlations [9,10] of 4_1^+ and 2_1^+ energies which give evidence for anharmonic vibrator and rotor behavior.

These studies [1–6] are both surprising and important, and potentially impact our understanding of the origins of some of the most characteristic features of nuclear spectra. Such features seem to emerge primarily from the nature of the basis space and the rank (2-body) of the interaction.

Despite all this recent work, there has been no explicit comparison with experiment. It is therefore one of the purposes of the present Letter to do so, with data on level energies spanning the entire nuclear chart [11]. This is the first time that detailed data on the low-lying nuclear spectra have been compared with predictions obtained from random ensembles. In the process, some previously unrecognized features of the data themselves will be discerned, which are not in fact produced with random interactions, giving us the kind of information needed to define favored interactions.

To proceed, we use two IBM Hamiltonian ensembles, the full, most general, Hamiltonian (denoted H_{IBM}) with two 1-body and seven 2-body interactions, and the more “focused” Hamiltonian $H_{\epsilon\kappa} = \epsilon n_d - \kappa Q \cdot Q$ of the extended consistent Q formalism (ECQF) [12,13], where $Q = s^\dagger \tilde{d} + d^\dagger s + \chi [d^\dagger \tilde{d}]^{(2)}$. We use either uniform, random $\chi \in [0, -\sqrt{7}/2]$ or fixed χ , as specified in each set of calculations below. The ensembles are defined by choosing random Gaussian interaction strengths in the Hamiltonians H_{IBM} and $H_{\epsilon\kappa}$ as in ref. [4]. The full Hamiltonian gives results essentially identical to those in Ref. [4], with peaks at $R_{4/2} \sim 2.0$ and 3.33 , and growing probability for the latter as N_B increases. The focused ECQF Hamiltonian (with random χ in the Q operator) gives similar but “cleaner” $R_{4/2}$ distributions. Both results are shown in the inset to Fig. 1. It is interesting to examine the correlations of $E(4_1^+)$ vs. $E(2_1^+)$. Empirically, this correlation has been shown [9,10] to be extremely robust, exhibiting a bi-modal character with slopes of 2.0 and 3.33 in collective nuclei. Comparisons of these data with calculations using the full H_{IBM} for boson number $N_B=16$ are shown in Fig. 1. The overall energy scale is fixed to the data by choosing the width of the Gaussian distributions. Similar results are obtained for other N_B .

While the overall agreement is excellent, the trends of Fig. 1 only show part of the story. They do not easily reveal the *density* distribution along the trajectory, that is, the probability distribution of nuclei as a *function* of $R_{4/2}$. And it is from this perspective that specific empirical features appear that are not described by calculations unless the range of interactions is constrained. To see this, consider Fig. 2(left) which shows empirical $R_{4/2}$ values for the entire nuclear chart from $Z=8-100$. In light nuclei, there is little evidence for collective $R_{4/2}$ values. In the lowest medium mass region, $28 < Z < 50$, however, a peak at $R_{4/2} \sim 2.3$ begins to emerge. In heavier nuclei this peak remains but is now accompanied by nuclei with larger $R_{4/2}$ values and, in particular, a sharp enhancement near $R_{4/2} \sim 3.33$. Fig 3a shows the composite distribution of $R_{4/2}$ values for all N_B . The peak at $R_{4/2} \sim 2.3$ persists.

Is this preference a fundamental feature of nuclear spectra or a result of some bias in the data? To study this we consider in Fig. 2(middle) a different cut through the available

$R_{4/2}$ data, namely, distributions for different ranges of boson numbers (i.e., valence nucleon numbers: $N_{val} = 2N_B$). Pre-collective nuclei ($N_B \leq 3$) show few $R_{4/2}$ values above 2.0. Nuclei with $N_B \geq 13$ are nearly all rotational, and those with N_B in the range of 4-12 are transitional. Surprisingly, no range of valence nucleon number shows an enhancement at $R_{4/2} \sim 2.0$, contrary to the results of the random ensembles. (In this context we recall that the slope of 2.0 in Fig. 1 does not imply $R_{4/2} = 2.0$ due to the finite intercept of this segment.) However, the second panel of Fig. 2(middle) shows that the peak centered on $R_{4/2} = 2.3$, mentioned above, is specifically associated with nuclei with 8 – 18 valence nucleons. To our knowledge, this striking feature has not been pointed out explicitly before but, as we shall see, leads to an empirical constraint on interactions that is not evident from Fig. 1 alone.

Part of the explanation of the shell-by-shell results in Fig. 2(left) therefore merely reflects changing shell sizes and hence the distribution of possible N_B values. However, this is not sufficient. It does not, for example, explain the overwhelming preference for rotational $R_{4/2}$ values in regions like $82 < Z < 102$ where nuclei with small numbers of valence nucleons also exist, or the abundance of $R_{4/2}$ values near 2.3 in the $50 < Z < 82$ shell. The data also reflect *which* nuclei are *known* in each region. For example, most known nuclei with $Z > 82$ have large N_B .

If we assume the universality of the empirical distributions in Fig. 2(middle), we can construct expected $R_{4/2}$ distributions for any region of nuclei simply by tallying the number of occurrences of a given N_B for a range of N and Z values and multiplying that number by the relevant empirical $R_{4/2}$ distribution. In Fig 3b, we show the $R_{4/2}$ distribution for all nuclei with $Z < 82$ assuming that, for each proton shell, all $R_{4/2}$ values are known for neutrons filling both the same shell and the next shell (regardless of where the drip lines are). So, for example, for $8 \leq Z < 20$, we compile the $R_{4/2}$ distribution for $8 \leq N < 28$. For $28 \leq Z < 50$, we use $28 \leq N < 82$. The peak at $R_{4/2} \sim 2.3$ persists, reflecting simply the fact that boson numbers from 4-9 appear frequently in virtually all shells. Fig. 3c shows similar results for $82 \leq Z < 126$ and $82 \leq N < 184$. The peak at $R_{4/2} \sim 2.3$ remains, but with a proliferation of larger boson numbers, a large abundance of rotational $R_{4/2}$ values near 3.33 also appears.

It is an important component of this Letter to see if calculations with random interactions can reproduce these $R_{4/2}$ distributions. Such calculations (for both H_{IBM} and $H_{\epsilon\kappa}$) are shown in Fig. 2(right) for comparison with the data in Fig. 2(middle). Some results agree with the empirical trends such as the lack of structure for low boson numbers with H_{IBM} and the abundance of $R_{4/2} \sim 3.33$ values for large N_B . However, these random calculations tend to give a peak at $R_{4/2} \sim 2$ and nowhere do they show a peak at 2.3.

We will see momentarily that this points towards the need for specific non-random interactions. First, though, it is important to note that, although the interactions used in $H_{\epsilon\kappa}$ are random, they actually contain an implicit bias in $R_{4/2}$ values. For $N_B = 7$ and ϵ/κ values from ∞ down to ~ 50 , IBM spectra are vibrational. For $\epsilon/\kappa \leq 20$ rotational spectra result. Thus, for a random interaction, which effectively samples an infinitely large range of ϵ/κ values, the measures of the vibrational and rotational regions far exceed that of the transitional region, which accounts for the high frequencies of calculated $R_{4/2}$ values near 2.0 and 3.33. (Similar arguments apply, but for shifted ranges of ϵ/κ , for the other N_B values.) The Gaussian random numbers also enhance the $O(6)$ values of $R_{4/2}$ (~ 2.5) for small N_B ,

as seen in Fig. 2 (right column, dashes).

We carried out a large sampling of calculations to determine the specific range of interactions that yield a given $R_{4/2}$ value and, in particular, $R_{4/2} \sim 2.3$ for $N_B = 4 - 9$. Figure 4 shows the statistical ranges of ϵ/κ and χ values that give $R_{4/2}$ in the ranges of 2.2-2.4 and 2.8 - 3.0 for $N_B=7$. Given the discussion just above, it is not surprising that $R_{4/2} \sim 2.3$ values require intermediate ranges of ϵ/κ near 20-30.

Thus, the empirical preference for $R_{4/2} \sim 2.3$ values reflects *two equally necessary* ingredients: the relevant interactions, and the *locus* of accessible nuclei. Had the valley of stability lain elsewhere, or had the ϵ/κ and χ values been different, the $R_{4/2}$ distribution would have been different. Comparison of measured $R_{4/2}$ distributions in new, unmapped regions with expectations (as in Figs. 3(b)-(c)) can thus be used to deduce information either on shell structure (e.g., magic numbers) or on the interactions applicable to these new nuclei.

Another example of characteristic nuclear data that constrains the interaction comes from rotational nuclei, namely, the energies of gamma vibrational modes, $E(2_2^+)$, in deformed nuclei. In Fig. 5a we show the results for H_{IBM} with $N_B = 16$ (to approximate the mean boson number for the deformed rare earth nuclei). There is no evidence for a peak in $R_{2/2} \equiv E(2_2^+)/E(2_1^+)$ at any value larger than 2. In heavy nuclei, however, such excitations are well known to occur at 10-20 times the 2_1^+ energy. Fig. 5b shows a collection of empirical results for $R_{2/2}$ for the rare earth region showing a broad bump centered on $R_{2/2} \sim 15$. If we now truncate the interaction space to that relevant for deformed nuclei, that is, $\epsilon/\kappa < 26$ we see, as shown in Fig. 5c, that, for each χ value, a distinct peak in $R_{2/2}$ probability appears. The peak for $\chi = -0.4$ (solid), which is the traditional value for deformed nuclei, gives an excellent reproduction of the data. Once again, therefore, specific data on actual nuclei help identify and constrain the nature and relative importance of the 1- and 2-body residual interactions.

To summarize, we presented a confrontation of the data for $Z=8-100$ with the predictions of nuclear structure calculations with random interactions, in the framework of the IBM. (a) General features of nuclear spectra, such as 0^+ ground states and the appearance of vibrational and rotational nuclei [4], and the global $E(4_1^+) vs. E(2_1^+)$ trajectory, are typical of calculations with random interactions; (b) Heretofore unrecognized features of the data such as the *absence* of an abundance peak at the vibrator value $R_{4/2} = 2.0$ and a frequency enhancement at $R_{4/2} \sim 2.3$, in nuclei with intermediate numbers of valence nucleons, were discovered. (c) Such robust features of nuclear data, or others such as the characteristic energies of γ -vibrational modes in deformed nuclei, point to specific ranges of interactions. In particular, we showed that data such as these depend *both* on the relevant valence nucleon numbers (i.e., the nuclei that are known) and on the interactions. If the residual interactions change in new nuclei (e.g., near the drip lines), then so will the distributions of $R_{4/2}$ values and the collective features of exotic nuclei. If the locus of newly accessible nuclei favors certain shell regions, the distribution of $R_{4/2}$ values and the nature of collective modes will reflect this as well. Conversely, valence nucleon number, and hence shell structure and the locations of magic nuclei, can be estimated from empirical knowledge of $R_{4/2}$ values, even when the magic nuclei themselves are not accessible. The usefulness of this result in studies of exotic nuclei, where issues of shell structure or the nature of residual interactions are paramount, is obvious.

We are grateful to Alejandro Frank, Roelof Bijker, Stuart Pittel and Franco Iachello for discussions that initiated and motivated this work. Work supported by the U.S. DOE under Grant numbers DE-FG02-91ER-40609, DE-FG02-91ER-40608, and DE-FG02-88ER40417.

- [1] C.W. Johnson, G.F. Bertsch, and D.J. Dean, Phys. Rev. Lett. **80**, 2749 (1998)
- [2] R. Bijker, A. Frank, and S. Pittel, Phys. Rev. **C60**, 021302 (1999)
- [3] C.W. Johnson, G.F. Bertsch, D.J. Dean, and I. Talmi, Phys. Rev. **C61**, 014311 (1999)
- [4] R. Bijker and A. Frank, Phys. Rev. Lett **84**, 420 (2000)
- [5] R. Bijker, A. Frank, and S. Pittel, nucl-th/0004032.
- [6] R. Bijker and A. Frank, nucl-th/0004002.
- [7] J.B. French et al., Phys. Rev. Lett. **54**, 2313 (1985)
- [8] I. Talmi, *Simple Models of Complex Nuclei* (Harwood Academic Publishers, Chur, 1993).
- [9] R.F. Casten, N.V. Zamfir, D.S. Brenner, Phys. Rev. Lett. **71**, 227 (1983).
- [10] N.V. Zamfir, R.F. Casten, Phys. Lett. **341B**, 1 (1994).
- [11] *Nuclear Data Sheets* through **87**, No. 1 (1999).
- [12] D.D. Warner and R.F. Casten, Phys. Rev. Lett. **48**, 1385 (1982).
- [13] P.O. Lipas, P. Toivonen, D.D. Warner, Phys. Lett. **155B**, 295 (1985).

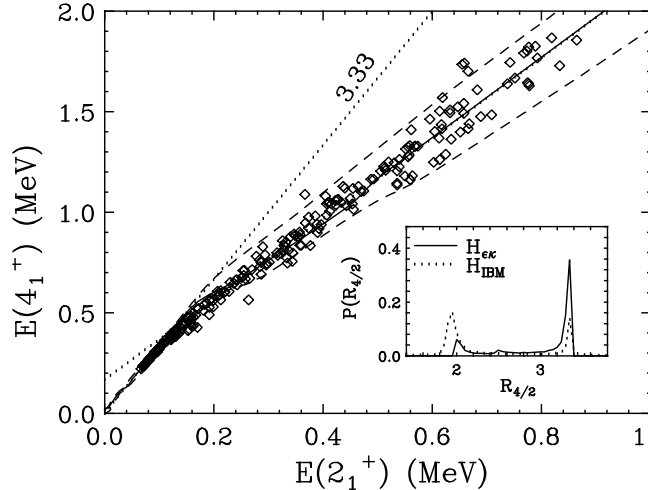


FIG. 1. Plot of $E(4_1^+)$ against $E(2_1^+)$ for collective nuclei with $38 < Z < 82$ (\diamond), similar to [9]. In this and the following figures, we use all available data from [11]. The data lie along lines with slopes 2.0 and 3.33 (dots). The finite intercept of the former implies $E(4_1^+) = E(2_1^+) + \epsilon$. Hence $R_{4/2} = 2 + \epsilon/E(2_1^+)$ varies along this segment. The statistical distribution of $E(4_1^+)$ and $E(2_1^+)$ energies for the full H_{IBM} is a strongly correlated function, whose maximum is indicated by the solid line, and the approximate FWHM by the dashes, which agrees well with the data. The variance of the Gaussian random numbers (which scales both axes) is adjusted to match the transition point between the two empirical slopes. (Inset) Statistical distribution of $R_{4/2}$ for the full Hamiltonian (dots) and $H_{\epsilon\kappa}$ (solid) showing peaks at 2.0 and 3.33. (In the main figure, the points corresponding to the abundance peak at $R_{4/2} \sim 2$ are at high $E(2_1^+)$, offscale at the upper right.) All simulations are for $N_B = 16$ and 50000 realizations of the random Hamiltonians.

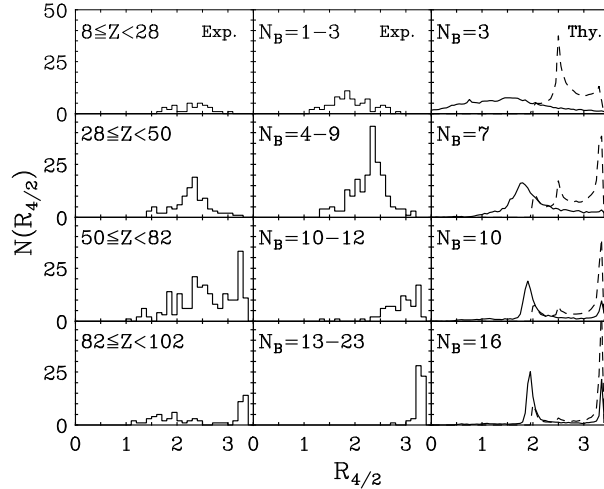


FIG. 2. (Left column) Experimental distribution of $R_{4/2}$ as a function of proton shells. (Middle column) Experimental distribution of $R_{4/2}$ as a function of N_B . (The number of valence nucleons is $2N_B$.) (Right column) Statistical predictions of $R_{4/2}$ for selected boson numbers using H_{IBM} (solid) and $H_{\epsilon\kappa}$ (dashes) with random χ . The vertical scale for this column is arbitrary.

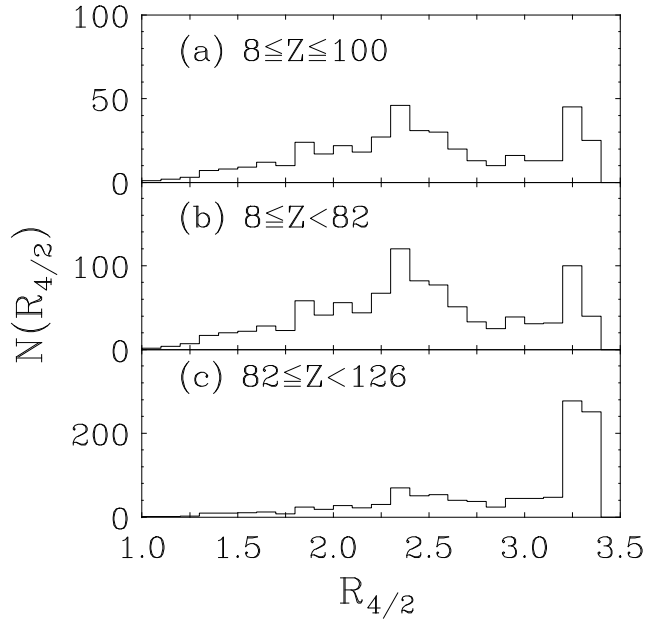


FIG. 3. Empirical distributions of $R_{4/2}$ for indicated proton regions. (a) Sum of existing data from Fig. 2(left). (b) and (c) Semi-empirical estimates of $R_{4/2}$ distributions for large regions of nuclei where it is assumed that the $R_{4/2}$ values would be available for full proton and neutron shells. Specifically, for each full proton shell, we take the set of nuclei obtained when the neutrons fill the same and next higher shell. These panels are constructed by assuming that the empirical distributions in Fig. 2 (middle) apply to all nuclei and, therefore, by folding these distributions with the frequency of N_B for these regions.

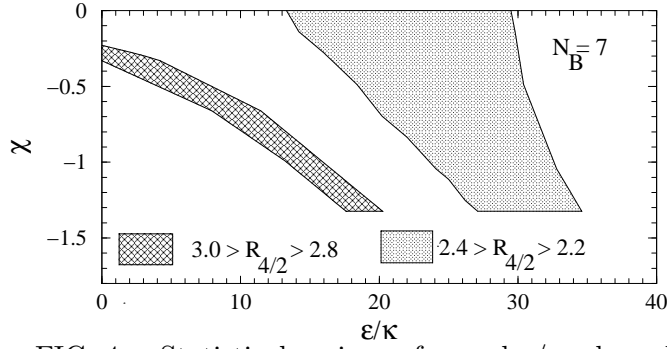


FIG. 4. Statistical regions of χ and ϵ/κ where $R_{4/2}$ falls in the range 2.2–2.4 and 2.8–3.0 for $N_B = 7$.

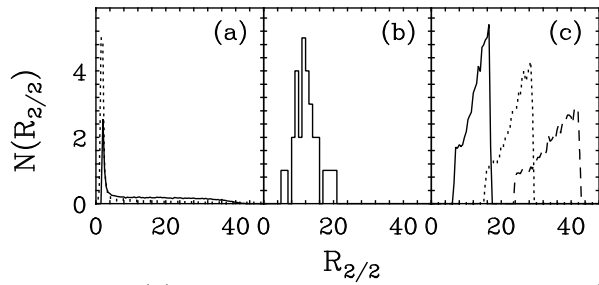


FIG. 5. (a) Distribution of $R_{2/2}$ for H_{IBM} (dots) and $H_{\epsilon\kappa}$ with random χ (solid). (b) Experimental distribution of $R_{2/2}$. (c) Distributions for $H_{\epsilon\kappa}$ for $\epsilon/\kappa < 26$ and $\chi = -\sqrt{7}/2$ (dashes), -0.8 (dots) and -0.4 (solid), showing the selectivity in $R_{2/2}$.